Numerical modeling of the interaction of light with nanometer scale structures

Stéphane Lanteri, Raphaël Léger and Jonathan Viquerat
NACHOS project-team, Inria Sophia Antipolis - Méditerranée, France
Claire Scheid
University of Nice - Sophia Antipolis
J.A. Dieudonné Laboratory UMR CNRS 7351, France

Fourth Workshop of the CNPq-Inria HOSCAR project
High Performance Computing and Scientific Data Management
Driven by Highly Demanding Applications
Universidade Federal do Rio Grande do Sul (UFRGS), Gramado, Brazil

History

- Created in July 2007
- Common project-team with J.A. Dieudonné (JAD) Mathematics Laboratory UMR CNRS 7351, University of Nice-Sophia Antipolis (UNSA)

Permanent staff

- INRIA
  - Loula Fezoui
  - Marie-Hélène Lallemand
  - Stéphane Lanteri
- JAD Laboratory, UNSA
  - Stéphane Descombes
- INRIA/UNSA Chair
  - Claire Scheid

Non-permanent staff (September 2014)

- 4 Ph.D students, 2 fixed-term engineers, 1 postdoc
- 1 long-term visitor (Frédéric Valentin, LNCC, Petropolis, Brazil)

Scientific objectives

- At first glance, a methodology-driven project-team
- Numerical modeling of physical problems involving waves in interaction with complex media and irregularly shaped structures
  - Systems of *linear* PDEs with variable coefficients
  - Time-domain and time-harmonic problems
- Methodological aspects
  - Theoretical (properties of numerical methods)
  - Practical (numerical algorithms and associated software)
- Application aspects
  - Focus on a few applications, preferably related to scientific and technological challenges of interest to the quality of life in our society
  - Contribute to a realistic numerical modeling of the underlying physical phenomena and demonstrate the benefits of the proposed methodologies

High order Discontinuous Galerkin (DG) methods

- Formulation and analysis of DG methods on simplicial and mixed cartesian-simplicial meshes
- High order polynomial interpolation
- Non-conformity (local *h*-, *p*- and *hp*-adaptivity)
- Numerical treatment of complex material models

Numerically efficient solution strategies

- Locally implicit time integration methods
- Domain decomposition methods

High performance computing

- Algorithmics for modern parallel computing platforms
- Hybrid MIMD-SIMD parallelization strategies
- Large-scale simulations

NACHOS project-team

Computational electromagnetics

- System of Maxwell equations
- Dispersive propagation media
- Applications involve the interaction of electromagnetic waves with,
  1. Biological tissues (biocem),
  2. Nanoscale objects (nanophotonics).

Computational geoseismics

- System of elastodynamic equations
- Viscoelastic propagation media
- Applications deal with the propagation of seismic waves,
  1. Generated by an explosive source (earthquake dynamics),
  2. In the subsurface (resource prospection).

Outline

Computational nanophotonics: some generalities

Modeling context

- Nanophotonics or nano-optics is the study of the behavior of light on the nanometer scale
- It is considered as a branch of optical engineering which deals with optics, or the interaction of light with particles or substances, at deeply subwavelength length scales
- Refers to phenomena of ultraviolet, visible and near IR light, with a wavelength of approximately 300 to 1200 nanometers
- The interaction of light with these nanoscale features leads to confinement of the electromagnetic field to the surface or tip of the nanostructure resulting in a region referred to as the optical near field

Modeling challenges

- Metal nanoparticles and metal/dielectric interfaces
- Very strong localized EM field enhancements
- Local, non-local and possibly non-linear dispersion effects

Computational nanophotonics: some generalities

Modeling context

- Nanophotonics or nano-optics is the study of the behavior of light on the nanometer scale
- It is considered as a branch of optical engineering which deals with optics, or the interaction of light with particles or substances, at deeply subwavelength length scales
- Refers to phenomena of ultraviolet, visible and near IR light, with a wavelength of approximately 300 to 1200 nanometers
- The interaction of light with these nanoscale features leads to confinement of the electromagnetic field to the surface or tip of the nanostructure resulting in a region referred to as the optical near field

Modeling challenges

- Metal nanoparticles and metal/dielectric interfaces
- Very strong localized EM field enhancements
- Local, non-local and possibly non-linear dispersion effects

A typical physical setting (nanoplasmonics)

- SPs are coherent electron oscillations at the interface between any two materials where the real part of the dielectric function changes sign across the interface
- SPs typically exists at a metal-dielectric interface
- When SPs couple with a photon, the resulting hybridized excitation is called a surface plasmon polariton (SPP)
- This SPP can propagate along the surface of a metal until energy is lost either via absorption in the metal or radiation into free space

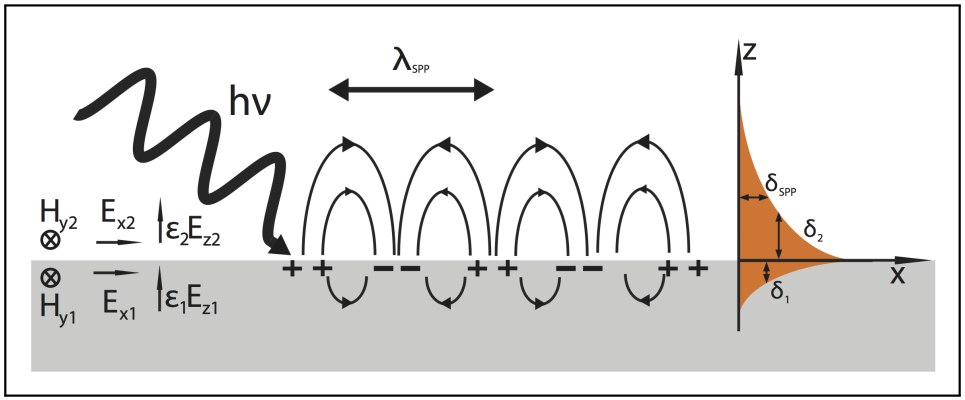

Schematic representation of an electron density wave propagating along a metal-dielectric interface. The exponential dependence of the electromagnetic field intensity on the distance away from the interface is shown on the right. These waves can be excited very efficiently with light in the visible range of the electromagnetic spectrum.

Applications

The enabling nature of nanophotonics means that the potential applications of nanophotonics are expected to be be broad.

Examples applications with potential commercial and/or societal impact are:

1. Nano-engineered photonics materials
2. Nanoscale quantum optics
3. Nanoscale functional imaging
4. Photovoltaics
5. Communications and all-optical signal processing
6. Chemical biosensors
7. Plasmon-enhanced magnetic storage

Applications: nanoscale functional imaging

Majour photonics needs

- Improved imaging tools for biologists, biochemists and materials scientists with 5-10 nm spatial resolution for individual proteins cell membrane manipulation, and more sophisticated interfaces for photo-induced life science processes
- Faster and more sensitive light detectors
- New probes/markers and assays suitable for nanoscale functional imaging (fluorophores, nanoantennas, surface enhanced Raman spectroscopy [SERS] substrates)
- Ultra-compact integrated systems for lab-on-chip applications

Applications: nanoscale functional imaging

The optical antenna concept is very promising for achieving ultrahigh spatial resolution and sensitivity, but requires development for real-world applications

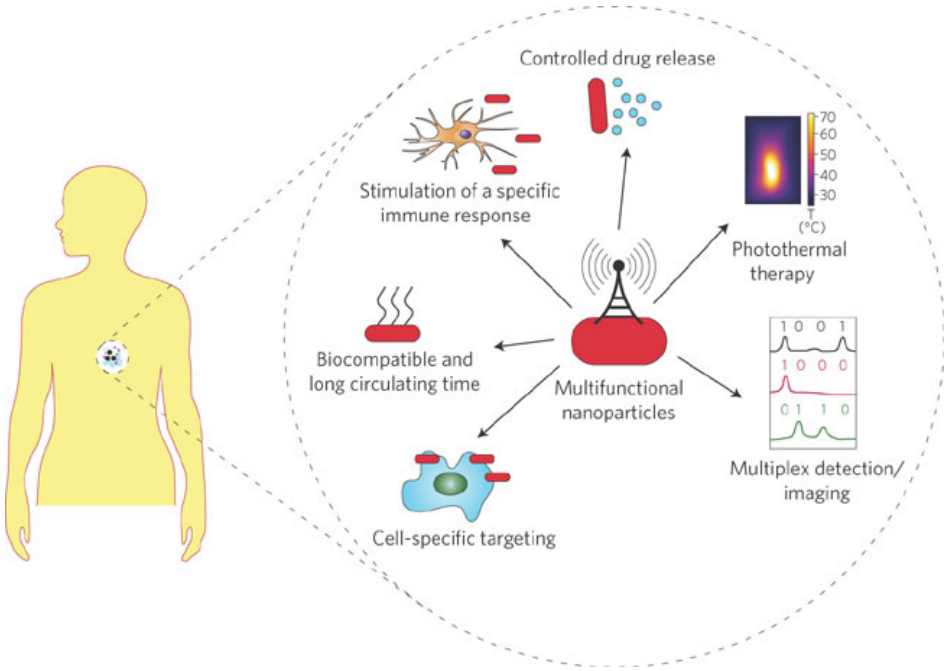

From: Tumour targeting: nanoantennas heat up
W. Zhao and J.M. Karp, Nature Materials 8, pp. 453-454, 2009

Computational nanophotonics: some generalities

- Challenges with the simulation of ElectroMagnetic (EM) wave propagation
  - Geometrical characteristics of the propagation domain:
    - dimensions relatively to the wavelength,
    - irregularly shaped objects and singularities.
  - Physical characteristics of the propagation medium:
    - heterogeneity and anisotropy,
    - physical dispersion and dissipation.
  - Characteristics of the radiating sources and incident fields
- PDE model: the system of Maxwell equations

James Clerk Maxwell (1831-1879)

Table of contents

Outline

- FDTD: Finite Difference Time-Domain method
- Seminal work of K.S. Yee
  (IEEE Trans. Antennas Propag., Vol. AP-14, 1966)
- Structured (cartesian) meshes
- Second order accurate (space and time) on uniform meshes
- Advantages
  - Easy computer implementation
  - Computationally efficient (very low algorithmic complexity)
  - Mesh generation is straightforward
  - Modelization of complex sources (antennas, thin wires, etc.) is well established
- Drawbacks
  - Accuracy on non-uniform discretizations
  - Memory requirements for high resolution models
  - Approximate discretization of boundaries (stair case representation)

Staircaising effect

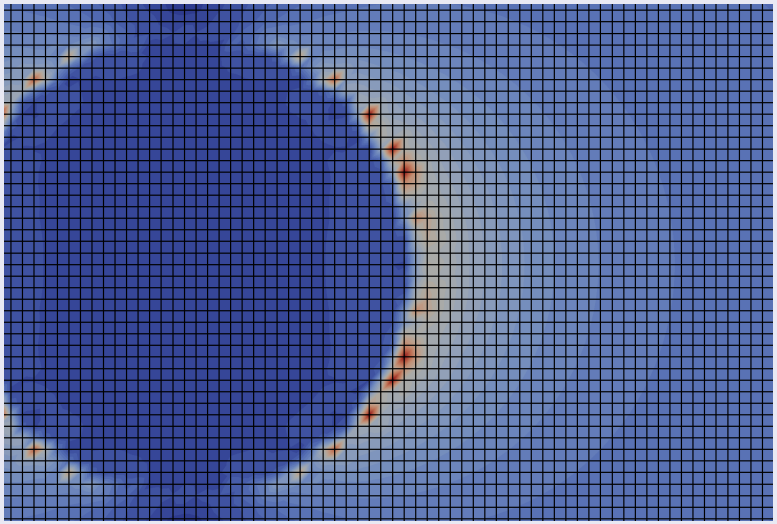

Simulation of the scattering of a plane wave by a nanosphere. Numerical illustration of the staircaising effect using a solution method on a uniform cartesian mesh.

- FETD: Finite Element Time-Domain method
- Often based on J.-C. Nédélec edge elements (Numer. Math, Vol. 35, 1980 and Vol. 50, 1986)
  - Unstructured meshes
  - Advantages
    - Accurate representation of complex shapes
    - Well suited to high order interpolation methods
  - Drawbacks
    - Computer implementation is less trivial
    - Unstructured mesh generation is hardly automated
    - Global mass matrix
  - Mass lumped FETD methods
    - S. Pernet, X. Ferrieres and G. Cohen
      IEEE Trans. Antennas Propag., Vol. 53, No. 9, 2005
    - Hexahedral meshes, high order Lagrange polynomials
    - Leap-frog time integration scheme

- FVTD: Finite Volume Time-Domain method
  - Imported from the CFD community
    - V. Shankar, W. Hall and A. Mohammadian
      Electromag. Vol. 10, 1990
    - J.-P. Cioni, L. Fezoui and H. Steve
      IMPACT Comput. Sci. Eng., Vol. 5, No. 3, 1993
    - P. Bonnet, X. Ferrieres *et al.*
      J. Electromag. Waves and Appl., Vol. 11, 1997
    - S. Piperno and M. Remaki and L. Fezoui
      SIAM J. Num. Anal., Vol. 39, No. 6, 2002.
  - Unstructured meshes
  - Uknowns are cell averages of the field components
  - Flux evaluation at cell interfaces
    - Upwind scheme $\rightarrow$ numerical dissipation
    - Centered scheme $\rightarrow$ numerical dispersion (on non-uniform meshes)
  - Extension to higher order accuracy: MUSCL technique

- DGTD: Discontinuous Galerkin Time-Domain method
  - F. Bourdel, P.A. Mazet and P. Helluy
    Proc. 10th Inter. Conf. on Comp. Meth. in Appl. Sc. and Eng., 1992.
    - Triangular meshes, first-order upwind DG method (i.e FV method)
    - Time-domain and time-harmonic Maxwell equations
  - M. Remaki and L. Fezoui, INRIA RR-3501, 1998.
    - Time-domain Maxwell equations
    - Triangular meshes, P1 interpolation, Runke-Kutta time integration (RKDG)
  - J.S. Hesthaven and T. Warburton (J. Comput. Phys., Vol. 181, 2002)
    - Tetrahedral meshes, high order Lagrange polynomials, upwind flux
    - Runge-Kutta time integration
  - B. Cockburn, F. Li and C.-W. Shu (J. Comput. Phys., Vol. 194, 2004)
    - Locally divergence-free RKDG formulation
  - G. Cohen, X. Ferrieres and S. Pernet (J. Comput. Phys., Vol. 217, 2006)
    - Hexahedral meshes, high order Lagrange polynomials, penalized formulation
    - Leap-frog time integration scheme
  - And a steadily increasing number of other works and groups adopting the method since 2005

Discontinuous Galerkin Time Domain method

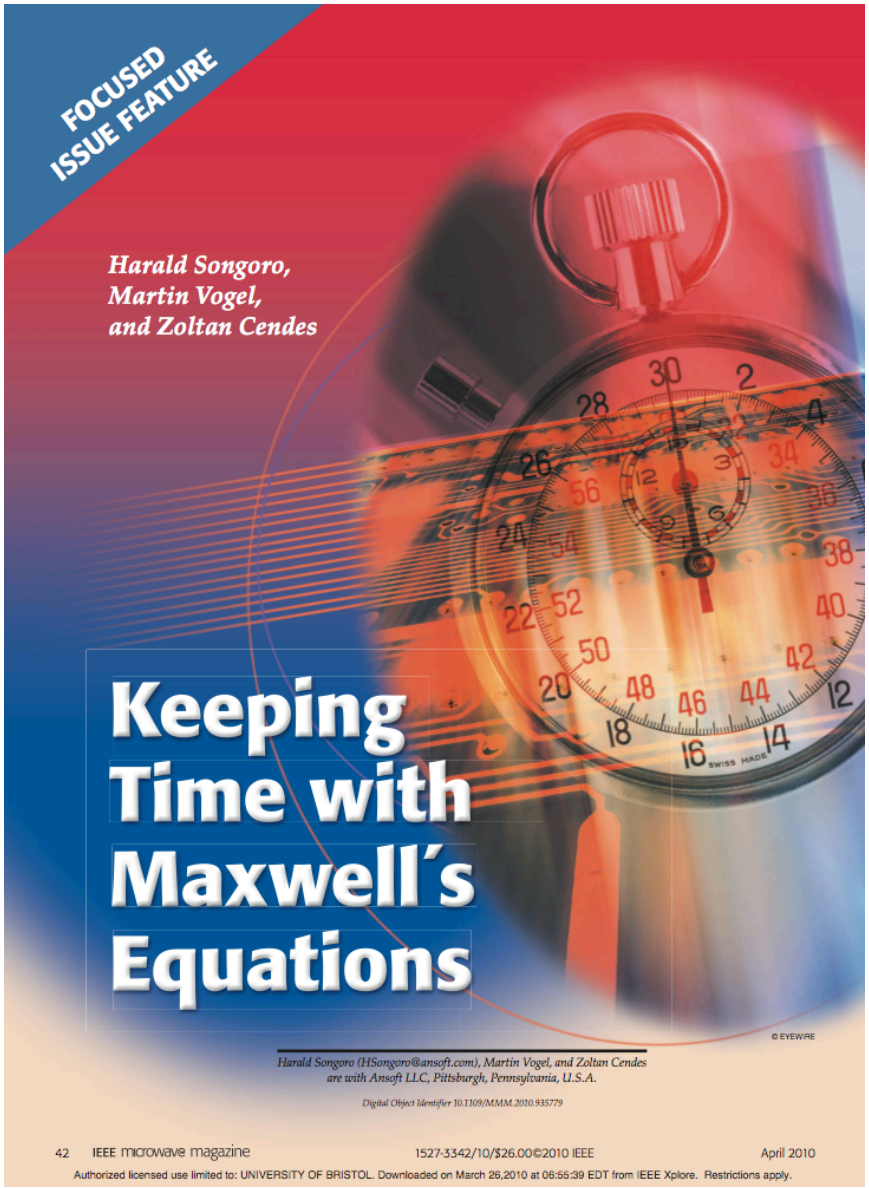

Introducing a commercial FETD solver breaks new ground in EM field simulation. Based on the DGTD method, it allows unstructured geometry-conforming meshes to be used for the first time in transient EM field simulation.

DGTD is a competitive alternative to traditional FDTD based methods to solving Maxwell's equations in the time domain. The applications presented here include the electromagnetic pulse susceptibility of the differential lines in a laptop computer, the radar signature of a landmine under undulating ground, the TDR of a bent flex circuit, and the return loss of a connector. All of these examples involve complicated, curved geometries where the flexibility of the unstructured meshes used in DGTD provides powerful advantages over simulation by conventional brick-shaped FDTD and FIT meshes.

IEEE Microwave Magazine - April 2010

- Problem to be solved

  $\mathbf{x} \in \Omega \subset \boldsymbol{R}^d$, $t \in \boldsymbol{R}^+$, $u = u(\mathbf{x}, t)$, $a_i = a_i(\mathbf{x})$ scalar real functions

$$\frac{\partial u}{\partial t} + \sum_{i=1}^{d} a_i \frac{\partial u}{\partial x_i} = 0$$

- Weak formulation

$$< \frac{\partial u}{\partial t}, \ v >_\Omega + \sum_{i=1}^{d} < a_i \frac{\partial u}{\partial x_i}, \ v >_\Omega = 0$$

$< u \ , \ v >_\Omega = \int_\Omega uv d\mathbf{x}$, v being a *test function*

- Galerkin method
  - $\tau_h = \{K\}$ triangulation of Ω
  - $\mathbb{P}_m(K)$: polynomials of degree at most m on K
  - Approximation space: $V_h = \{v^h \in L^2(\Omega) \mid \forall K \in \tau_h, \quad v^h|_K \equiv v_K \in \mathbb{P}_m(K)\}$

For each $K \in \tau_h$ find $u^h \in V_h$ such that:

$$< \frac{\partial u^h}{\partial t}, \ v >_K + \sum_{i=1}^{d} < a_i \frac{\partial u^h}{\partial x_i}, \ v >_K = 0 \ \ , \forall v \in P^m(K)$$

Integrating by parts (setting $a|_K \in \mathbb{P}_0(K)$):

$$\begin{aligned} < \frac{\partial u^h}{\partial x_i}, \ v >_K \quad &= \quad - < u^h, \ \frac{\partial v}{\partial x_i} >_K + < u^h n_i, \ v >_{\partial K} \\ < u, \ v >_{\partial K} \quad &= \quad \sum_{j=1}^{N_f(K)} {}_{\partial K \cap \partial K_j} \end{aligned}$$

  - $\mathbf{n} = \{n_i\}$ outward unit normal of ∂K
  - $N_f(K) =$ number of faces of K

- Discontinous approximation: $u^h|_{K\cap K_j}$ not well defined!
  $\Rightarrow$ Centered (or upwind) numerical fkux (numerical trace)
- Linear algebra
  - $u^h|_K(\mathbf{x},t) = \sum_{j=1}^{m_K} u^h_{j,K}(t)\psi_{j,K}(\mathbf{x}) \;\;,\;\; m_K = \dim(\mathbb{P}_m(K))$
  - $\{\psi_{j,K}\}, j = 1,\ldots,m_K$: basis of $\mathbb{P}_m(K)$

$$\mathbf{M}_K \frac{\partial \mathbf{U}^h_K}{\partial t} = \sum_{i=1}^{d} a_i \left(\mathbf{R}_{i,K}\mathbf{U}^h_K - n_i \sum_{j=1}^{N_f(K)} \mathbf{S}_{K,K_j} \left(\frac{\mathbf{U}^h_K + \mathbf{U}^h_{K_j}}{2} \right) \right)$$

$$\left\{ \begin{array}{lcl} \mathbf{U}^h_K & = & \mathbf{U}^h_K(t) = \{u^h_{j,K}(t)\}, \;\; j = 1,\ldots,m_K \\ \mathbf{M}_K[l,m] & = & < \psi_{l,K},\; \psi_{m,K} >_K \\ \mathbf{R}_{i,K}[l,m] & = & < \dfrac{\partial \psi_{l,K}}{\partial x_i},\; \psi_{m,K} >_K \\ \mathbf{S}_{K,K_j}[l,m] & = & < \psi_{l,K},\; \psi_{m,K_j} >_{\partial K\cap\partial K_j} \end{array} \right.$$

Dimension of local systems: $m_K \times m_K$

Context and objectives of our work

Objectives and planned contributions

- Development of a high order DGTD method for nanophotonics/nanoplasmonics
- System of 3D Maxwell equations + material models
- Geometry conforming mesh
- High order collocated interpolation of the physical fields
- High performance computing-enabled numerical kernels
- Study of numerical analysis issues (stability, convergence)
- Implementation in a dedicated software
- Validation and evaluation conducted in collaboration with potential users

Starting point

- DGTD method for the system of 3D Maxwell equations [2003-2012]
- Non-dispersive media
- Extensiveley developed for microwave/RF applications

Outline

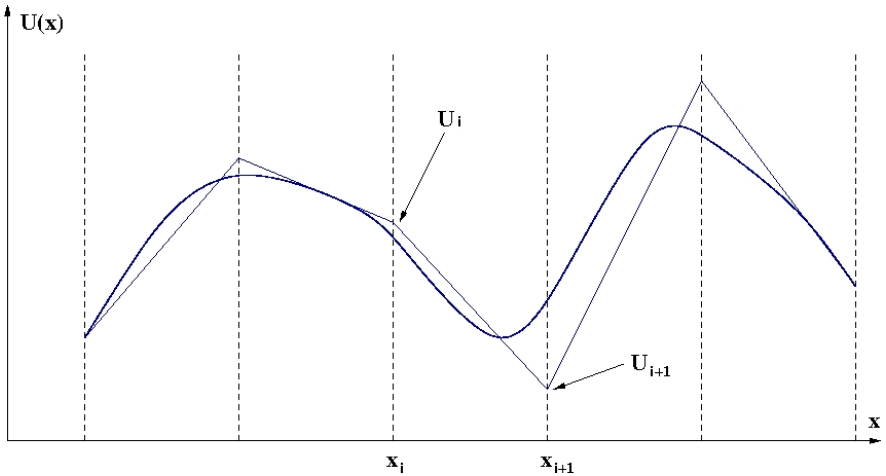

Continuous P1 interpolation

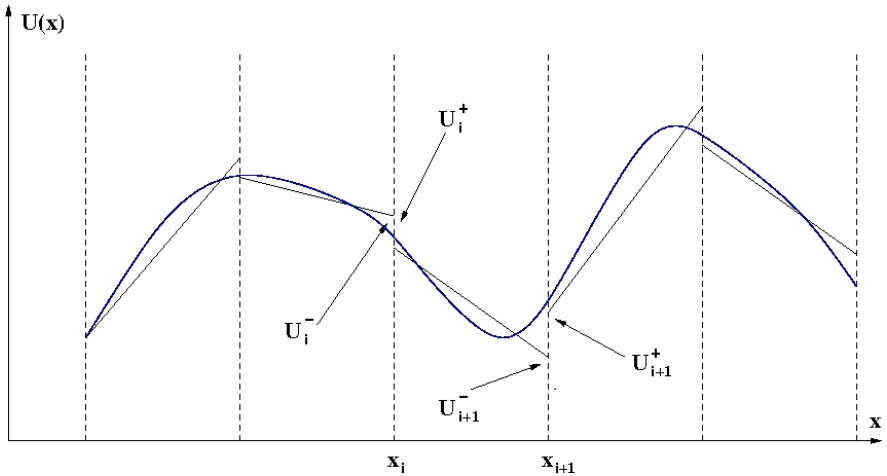

Discontinuous P1 interpolation

- Naturally adapted to heterogeneous media and discontinuous solutions
- Can easily deal with unstructured, possibly non-conforming meshes (*h*-adaptivity)
- High order with compact stencils and non-conforming approximations (*p*-adaptivity)
- Usually rely on polynomial interpolation but can also accomodate alternative functions (e.g plane waves)
- Yield block diagonal mass matrices when coupled to explicit time integration schemes
- Amenable to efficient parallelization
- But leads to larger problems compared to continuous finite element methods

DG for electromagnetic wave propagation in heterogeneous media

- Heterogeneity is ideally treated at the element level
  - Discontinuities occur at material (i.e element) interfaces
  - Mesh generation process is simplified
- Wavelength varies with ε and μ
  - For a given mesh density, approximation order can be adapted at the element level in order to fit to the local wavelength

Discretization of irregularly shaped domains

- Unstructured simplicial meshes
- The basic support of the DG method is the element (triangle in 2D and tetrahedron in 3D)
- Local refinement is facilitated by allowing non-conformity
- Non-conformity opens the route to the coupling of different discretization methods (e.g structured/unstructured)

Maxwell equations, $\mathbf{x} \in \Omega$, $t > 0$

$$\begin{cases} \varepsilon \partial_t \mathbf{E} - \nabla \times \mathbf{H} = 0 \\ \\ \mu \partial_t \mathbf{H} + \nabla \times \mathbf{E} = 0 \end{cases}$$

$$\mathbf{E} = \mathbf{E}(\mathbf{x}, t) \quad \text{and} \quad \mathbf{H} = \mathbf{H}(\mathbf{x}, t)$$

Boundary conditions: $\partial\Omega = \Gamma_a \cup \Gamma_m$

$$\begin{cases} \mathbf{n} \times \mathbf{E} = 0 \text{ on } \Gamma_m \text{ (metallic boundary)} \\ \mathbf{n} \times \mathbf{E} - \sqrt{\frac{\mu}{\varepsilon}} \mathbf{n} \times (\mathbf{H} \times \mathbf{n}) = \mathbf{n} \times \mathbf{E}_{\text{inc}} - \sqrt{\frac{\mu}{\varepsilon}} \mathbf{n} \times (\mathbf{H}_{\text{inc}} \times \mathbf{n}) \text{ on } \Gamma_a \text{ (absorbing boundary)} \end{cases}$$

where $(\mathbf{E}_{\text{inc}}, \mathbf{H}_{\text{inc}})$ is a given incident field.

Initial conditions

$$\mathbf{E}_0 = \mathbf{E}(\mathbf{x}, 0) \quad \text{and} \quad \mathbf{H}_0 = \mathbf{H}(\mathbf{x}, 0)$$

- Triangulation of Ω: $\overline{\Omega}_h \equiv \mathcal{T}_h = \bigcup_{\tau_i \in \mathcal{T}_h} \overline{\tau}_i$
  - $\mathcal{F}_0$: set of purely internal faces
  - $\mathcal{F}_m$ and $\mathcal{F}_a$: sets of faces on the boundaries Γ_m and Γ_a
- Approximation space: $V_h = \{\mathbf{V}_h \in L^2(\Omega)^3 \mid \forall i, \mathbf{V}_{h|\tau_i} \equiv \mathbf{V}_i \in \mathbb{P}_{p_i}(\tau_i)^3\}$
- Variational formulation: $\forall \vec{\varphi} \in \mathcal{P}_i = \mathrm{Span}(\vec{\varphi}_{ij}\ ,\ 1 \leq j \leq d_i)$

$$\left\{ \begin{array}{rcl} \displaystyle\iiint_{\tau_i} \vec{\varphi} \cdot \varepsilon_i \partial_t \mathbf{E} d\omega & = & \displaystyle -\iint_{\partial\tau_i} \vec{\varphi} \cdot (\mathbf{H} \times \vec{n}) ds + \iiint_{\tau_i} \nabla \times \vec{\varphi} \cdot \mathbf{H} d\omega \\ \displaystyle\iiint_{\tau_i} \vec{\varphi} \cdot \mu_i \partial_t \mathbf{H} d\omega & = & \displaystyle \iint_{\partial\tau_i} \vec{\varphi} \cdot (\mathbf{E} \times \vec{n}) ds - \iiint_{\tau_i} \nabla \times \vec{\varphi} \cdot \mathbf{E} d\omega \end{array} \right.$$

- Approximate fields: $\forall i$, $\mathbf{E}_{h|\tau_i} \equiv \mathbf{E}_i$ and $\mathbf{H}_{h|\tau_i} \equiv \mathbf{H}_i$
- But traces $\mathbf{E}_{h|\partial\tau_i \cap \partial\tau_j}$ and $\mathbf{H}_{h|\partial\tau_i \cap \partial\tau_j}$ are undefined!
- Introduce and appropriate treatment on the face $a_{ij} = \tau_i \cap \partial\tau_j$
- In the context of finite volume methods, this leads to the notion of numerical flux

$$\text{Centered flux} \quad : \quad \mathcal{F}(\mathbf{W}, \mathbf{n})|_{a_{ij}} = \mathbf{n} \cdot F(\frac{\mathbf{W}_i + \mathbf{W}_j}{2}) = G_{\mathbf{n}} \left(\frac{\mathbf{W}_i + \mathbf{W}_j}{2} \right)$$

$$\text{Upwind flux} \quad : \quad \mathcal{F}(\mathbf{W}, \mathbf{n})|_{a_{ij}} = G_{\mathbf{n}}^{+} \mathbf{W}_i + G_{\mathbf{n}}^{-} \mathbf{W}_j$$

- The choice of the numerical flux impacts the stability and the convergence of the scheme

- Integral over $\partial\tau_i$: $\mathbf{E}_{|a_{ik}} = \dfrac{\mathbf{E}_i + \mathbf{E}_k}{2}$ and $\mathbf{H}_{|a_{ik}} = \dfrac{\mathbf{H}_i + \mathbf{H}_k}{2}$ (i.e. centered flux)
- Assume $\Gamma_a = \emptyset$ (to simplify the presentation) and on Γ_m: $\mathbf{E}_{k|a_{ik}} = -\mathbf{E}_{i|a_{ik}}$ and $\mathbf{H}_{k|a_{ik}} = \mathbf{H}_{i|a_{ik}}$

$$\left\{\begin{array}{rcl}
\displaystyle\iiint_{\tau_i} \vec{\varphi}\cdot\varepsilon_i\partial_t\mathbf{E}_i d\omega & = & \displaystyle\frac{1}{2}\iiint_{\tau_i}(\nabla\times\vec{\varphi}\cdot\mathbf{H}_i + \nabla\times\mathbf{H}_i\cdot\vec{\varphi})d\omega \\
 & - & \displaystyle\frac{1}{2}\sum_{k\in\mathcal{V}_i}\iint_{a_{ik}}\vec{\varphi}\cdot(\mathbf{H}_k\times\vec{n}_{ik})ds \\
\displaystyle\iiint_{\tau_i} \vec{\varphi}\cdot\mu_i\partial_t\mathbf{H}_i d\omega & = & \displaystyle-\frac{1}{2}\iiint_{\tau_i}(\nabla\times\vec{\varphi}\cdot\mathbf{E}_i + \nabla\times\mathbf{E}_i\cdot\vec{\varphi})d\omega \\
 & + & \displaystyle\frac{1}{2}\sum_{k\in\mathcal{V}_i}\iint_{a_{ik}}\vec{\varphi}\cdot(\mathbf{E}_k\times\vec{n}_{ik})ds
\end{array}\right.$$

- Local projections

$$\mathbf{E}_i(\mathbf{x}) = \sum_{1\leq j\leq d_i} E_{ij}\vec{\varphi}_{ij}(\mathbf{x}) \quad \text{and} \quad \mathbf{H}_i(\mathbf{x}) = \sum_{1\leq j\leq d_i} H_{ij}\vec{\varphi}_{ij}(\mathbf{x})$$

- Vector representation of local fields

$$\mathbb{E}_i = \{E_{ij}\}_{1\leq j\leq d_i} \text{ and } \mathbb{H}_i = \{H_{ij}\}_{1\leq j\leq d_i}$$

- For $1 \leq j, l \leq d_i$:
  - $(\mathbf{M}_i^{\varepsilon})_{jl} = \varepsilon_i \iiint_{\tau_i} {}^{\mathsf{T}}\vec{\varphi}_{ij}\vec{\varphi}_{jl}\, d\omega \quad \text{and} \quad (\mathbf{M}_i^{\mu})_{jl} = \mu_i \iiint_{\tau_i} {}^{\mathsf{T}}\vec{\varphi}_{ij}\vec{\varphi}_{jl}\, d\omega$
  - $(\mathbf{K}_i)_{jl} = \frac{1}{2}\iiint_{\tau_i} ({}^{\mathsf{T}}\vec{\varphi}_{ij}\nabla\times\vec{\varphi}_{il} + {}^{\mathsf{T}}\vec{\varphi}_{il}\nabla\times\vec{\varphi}_{ij})\, d\omega$

- For $1 \leq j \leq d_i \quad \text{and} \quad 1 \leq l \leq d_k$
  - $(\mathbf{S}_{ik})_{jl} = \frac{1}{2}\iint_{a_{ik}} {}^{\mathsf{T}}\vec{\varphi}_{ij}(\vec{\varphi}_{kl}\times\vec{n}_{ij})\, ds$

Local EDO systems

$$\forall \tau_i \quad : \quad \begin{cases} \mathbf{M}_i^{\varepsilon} \dfrac{d\mathbb{E}_i}{dt} & = & \mathbf{K}_i \mathbb{H}_i & - & \displaystyle\sum_{k \in \mathcal{V}_i} \mathbf{S}_{ik} \mathbb{H}_k \\ \mathbf{M}_i^{\mu} \dfrac{d\mathbb{H}_i}{dt} & = & -\mathbf{K}_i \mathbb{E}_i & + & \displaystyle\sum_{k \in \mathcal{V}_i} \mathbf{S}_{ik} \mathbb{E}_k \end{cases}$$

Global EDO system (with $d = \sum_i d_i$ and metallic boundary only)

$$\mathbf{M}^{\varepsilon} \frac{d\mathbb{E}}{dt} = \mathbf{G}\mathbb{H} \quad \text{and} \quad \mathbf{M}^{\mu} \frac{d\mathbb{H}}{dt} = -{}^{\mathsf{T}}\mathbf{G}\mathbb{E}$$

- $\mathbf{G} = \mathbf{K} - \mathbf{A} - \mathbf{B}$
- $\mathbf{M}^{\varepsilon}$ are $\mathbf{M}^{\mu}$ block diagonal symmetric definite positive matrices
- $\mathbf{K}$ is a $d \times d$ block diagonal symmetric matrix
- $\mathbf{A}$ is a $d \times d$ block sparse symmetric matrix (internal faces)
- $\mathbf{B}$ is a $d \times d$ block sparse skew symmetric matrix (metallic faces)

- L. Fezoui, S. Lanteri, S. Lohrengel and S. Piperno
  ESAIM: M2AN, Vol. 39, No. 6, 2005
  Second order leap-frog time integration scheme, centered fluxes

Formulation: 2nd order Leap-Frog

$$\begin{cases} \mathbf{M}^{\varepsilon}\left(\dfrac{\mathbb{E}^{n+1}-\mathbb{E}^{n}}{\Delta t}\right) & = & \mathbf{G}\mathbb{H}^{n+\frac{1}{2}} \\ \mathbf{M}^{\mu}\left(\dfrac{\mathbb{H}^{n+\frac{1}{2}}-\mathbb{H}^{n-\frac{1}{2}}}{\Delta t}\right) & = & -{}^{\mathsf{T}}\mathbf{G}\mathbb{E}^{n+1} \end{cases}$$

Stability analysis

- Discrete electromagnetic energy

$$\mathcal{E}^{n} = {}^{\mathsf{T}}\mathbb{E}^{n}\mathbf{M}^{\varepsilon}\mathbb{E}^{n} + {}^{\mathsf{T}}\mathbb{H}^{n+\frac{1}{2}}\mathbf{M}^{\mu}\mathbb{H}^{n-\frac{1}{2}}$$

- Condition for $\mathcal{E}^{n}$ being a positive definite form

$$\Delta t \leq \frac{2}{d_2}, \quad \text{with} \quad d_2 = \| \, (\mathbf{M}^{-\mu})^{\frac{1}{2}} \; {}^{\mathsf{T}}\mathbf{G} \; (\mathbf{M}^{-\varepsilon})^{\frac{1}{2}} \, \|$$

- Higher order leap-frog time schemes
  H. Fahs and S. Lanteri
  J. Comput. Appl. Math., Vol. 234,2010
- Locally implicit time schemes
  V. Dolean, H. Fahs, L. Fezoui and S. Lanteri
  J. Comput. Phys., Vol. 229, No. 2, 2010

  L. Moya, S. Descombes and S. Lanteri
  J. Sci. Comp., Vol. 56, No. 1, 2013
- Non-conforming triangular meshes
  H. Fahs
  Numer. Math. Theor. Meth. Appl., Vol. 2, No. 3, 2009
- Hybrid structured/unstructured meshes
  C. Durochat, S. Lanteri and C. Scheid
  Appl. Math. Comput., Vol. 224, 2013

  C. Durochat, S. Lanteri and R. Léger
  Int. J. Numer. Model., Electron. Netw. Devices Fields, Vol. 27, No. 3, 2014

Outline

DGTD in nanophotonics

- Extensively developed in the recent years
- Theoretical Optics and Photonics group, Humboldt-Universität zu Berlin
  - K. Busch, M. König and J. Niegemann
    Discontinuous Galerkin methods in nanophotonics
    Laser and Photonics Reviews, Vol. 5, No. 6, 2011
  - M. König, K. Busch and J. Niegemann
    The discontinuous Galerkin time-domain method for Maxwell's equations with anisotropic materials
    Photonics and Nanostructures - Fundamentals and Applications, Vol. 8, 2010
- Theoretical Electrical Engineering Group in Paderborn University
  - Y. Grynko, J. Förstner and T. Meier
    Application of the discontinous Galerkin time domain method to the optics of metallic nanostructures
    AAPP— Physical, Mathematical, and Natural Sciences, Vol. 89 (S1), 2011
- TU Dresden, Institut für Angewandte Photophysik
  - A. Hille, R. Kullock, S. Grafström and L. M. Eng
    Improving nano-optical simulations through curved elements implemented within the discontinuous Galerkin method
    J. Comput. Theor. Nanos., Vol. 7, 2010

The Drude dispersion model

- Associated to a particularly simple theory that, for a chosen specific frequency range of interest and a given metallic material, models the optical and thermal properties of the latter
- The metal is considered as a static lattice of positive ions immersed in a free electrons gas
- Those electrons are considered to be the valence electrons of each metallic atom, that got delocalized when put into contact with the potential produced by the rest of the lattice atoms
- Frequency dependent permittivity is given by $\varepsilon_r(\omega) = \varepsilon_\infty - \frac{\omega_d^2}{\omega^2 + i\omega\gamma_d}$
- ε_∞ represents the core electrons contribution to the relative permittivity ε_r
- γ_d is a coefficient linked to the electron/ion collisions representing the friction experienced by the electrons
- $\omega_d = \sqrt{\frac{n_e e^2}{m_e \varepsilon_0}}$ (m_e is the electron mass, e the electronic charge and n_e the electronic density) is the plasma frequency of the electrons

The time-domain Maxwell-Drude equations

$$\begin{cases} \partial_t \mathbf{B} + \nabla \times \mathbf{E} = 0 \\ \\ \partial_t \mathbf{D} - \nabla \times \mathbf{H} = 0 \end{cases}$$

with the constitutive equations:

$$\begin{cases} \mathbf{D} = \varepsilon_0 \varepsilon_\infty \mathbf{E} + \mathbf{P} \\ \\ \mathbf{B} = \mu_0 \mathbf{H} \end{cases}$$

- Electric and magnetic fields: $\mathbf{E} = \mathbf{E}(\mathbf{x}, t)$ and $\mathbf{H} = \mathbf{H}(\mathbf{x}, t)$
- Electric displacement and magnetic induction: $\mathbf{D} = \mathbf{D}(\mathbf{x}, t)$ and $\mathbf{B} = \mathbf{B}(\mathbf{x}, t)$
- Electric polarization: $\mathbf{P} = \mathbf{P}(\mathbf{x}, t)$

The time-domain Maxwell-Drude equations

$$\begin{cases} \mu_0 \partial_t \mathbf{H} + \nabla \times \mathbf{E} = 0 \\ \\ \varepsilon_0 \varepsilon_\infty \partial_t \mathbf{E} + \partial_t \mathbf{P} - \nabla \times \mathbf{H} = 0 \end{cases}$$

- In the frequency domain, the polarization $\mathbf{P}$ is linked to the electric field through the relation $\hat{\mathbf{P}} = -\dfrac{\varepsilon_0 \omega_d^2}{\omega^2 + i\gamma_d \omega} \hat{\mathbf{E}}$
- Time domain ODE for the polariaztion

$$\frac{\partial^2 \mathbf{P}}{\partial t^2} + \gamma_d \frac{\partial \mathbf{P}}{\partial t} = \varepsilon_0 \omega_d^2 \mathbf{E}$$

- Dipolar current vector: $\mathbf{J}_p = \dfrac{\partial \mathbf{P}}{\partial t}$

The time-domain Maxwell-Drude equations

$$\begin{cases} \partial_t \mathbf{H} = -\nabla \times \mathbf{E} \\ \varepsilon_\infty \partial_t \mathbf{E} = \nabla \times \mathbf{H} - \mathbf{J}_p \\ \partial_t \mathbf{J}_p + \gamma_d \mathbf{J}_p = \omega_d^2 \mathbf{E} \end{cases}$$

Boundary condition: $\partial\Omega = \Gamma_a$

$$\mathbf{n} \times \mathbf{E} - \sqrt{\frac{\mu}{\varepsilon}} \mathbf{n} \times (\mathbf{H} \times \mathbf{n}) = \mathbf{n} \times \mathbf{E}_{\text{inc}} - \sqrt{\frac{\mu}{\varepsilon}} \mathbf{n} \times (\mathbf{H}_{\text{inc}} \times \mathbf{n}) \text{ on } \Gamma_a \text{ (absorbing boundary)}$$

where $(\mathbf{E}_{\text{inc}}, \mathbf{H}_{\text{inc}})$ is a given incident field.

Initial conditions

$$\mathbf{E}_0 = \mathbf{E}(\mathbf{x}, 0) \quad , \quad \mathbf{H}_0 = \mathbf{H}(\mathbf{x}, 0) \quad \text{and} \quad \mathbf{J}_{p,0} = \mathbf{J}_p(\mathbf{x}, 0)$$

ADE-DGTD method based on centered numerical fluxes

$$\left\{\begin{array}{lcl}
\mathbf{M}_i\left(\dfrac{\mathbb{H}_i^{n+\frac{3}{2}}-\mathbb{H}_i^{n+\frac{1}{2}}}{\Delta t}\right) & = & -\mathbf{K}_i\mathbb{E}_i^{n+1}+\displaystyle\sum_{k\in\mathcal{V}_i}\mathbf{S}_{ik}\mathbb{E}_k^{n+1} \\[2ex]
\mathbf{M}_i^{\varepsilon_\infty}\left(\dfrac{\mathbb{E}_i^{n+1}-\mathbb{E}_i^{n}}{\Delta t}\right) & = & \mathbf{K}_i\mathbb{H}_i^{n+\frac{1}{2}}-\displaystyle\sum_{k\in\mathcal{V}_i}\mathbf{S}_{ik}\mathbb{H}_k^{n+\frac{1}{2}}-\mathbf{M}_i\mathbb{J}_i^{n+\frac{1}{2}} \\[2ex]
\dfrac{\mathbb{J}_i^{n+\frac{3}{2}}-\mathbb{J}_i^{n+\frac{1}{2}}}{\Delta t} & = & \omega_d^2\mathbb{E}_i^{n+1}-\dfrac{\gamma_d}{2}\left(\mathbb{J}_i^{n+\frac{3}{2}}+\mathbb{J}_i^{n+\frac{1}{2}}\right)
\end{array}\right.$$

ADE-DGTD method based on centered numerical fluxes: stability analysis

J. Viquerat, M. Klemm, S. Lanteri and C. Scheid
http://hal.inria.fr/hal-00819758

- Discrete electromagnetic energy for the cell T_i

$$\xi_i^n = \frac{1}{2}\left(\int_{T_i} \mathbf{H}_i^{n+\frac{1}{2}} \cdot \mathbf{H}_i^{n-\frac{1}{2}} + \varepsilon_\infty \int_{T_i} \mathbf{E}_i^n \cdot \mathbf{E}_i^n + \frac{1}{\omega_d^2}\int_{T_i} \mathbf{J}_i^{n+\frac{1}{2}} \cdot \mathbf{J}_i^{n-\frac{1}{2}}\right)$$

- Total energy at a given time $t_n = n\Delta t$: $\xi^n = \sum_{i=0}^{N_T} \xi_i^n$
- The fully discrete ADE-DGTD scheme is stable under the CFL condition,

$$\Delta t < \min\left(\frac{h}{C}, \frac{2}{\omega_d + \gamma_d}, \frac{4\varepsilon_\infty}{\frac{C}{h} - \omega_d}\right)$$

- Under CFL condition, the discrete energy ξ^n can be bounded as,

$$\xi^n \leq \frac{\xi^0}{\left(\frac{1-\theta}{1+\theta}\right)^n}, \forall n \in \mathbb{N}^* \quad \text{with } \theta \geq 0$$

ADE-DGTD method based on centered numerical fluxes: a priori convergence

J. Viquerat, M. Klemm, S. Lanteri and C. Scheid
http://hal.inria.fr/hal-00819758

Let $(\mathbf{H}, \mathbf{E}, \mathbf{J}_p) \in \mathcal{C}^3\left([0, T], L^2(b\Omega)^9\right) \bigcap \mathcal{C}^0\left([0, T], H^{s+1}(\Omega)^9\right)$

Under the CFL condition the following error estimate holds,

$$\max_{n\in[0,N]} \left(\left\| \mathbf{H}\left(t_{n+\frac{1}{2}}\right) - \mathbf{H}_h^{n+\frac{1}{2}} \right\|^2_{L^2(\Omega)^3} + \|\mathbf{E}(t_n) - \mathbf{E}_h^n\|^2_{L^2(\Omega)^3} + \left\| \mathbf{J}_p\left(t_{n+\frac{1}{2}}\right) - \mathbf{J}_h^{n+\frac{1}{2}} \right\|^2_{L^2(\Omega)^3} \right)^{\frac{1}{2}}$$
$$\leq C\left(\Delta t^2 + h^{\min(s,k)}\right)\left(\|(\mathbf{H}, \mathbf{E}, \mathbf{J}_p)\|_{\mathcal{C}^3([0,T],L^2(\Omega)^9)} + \|(\mathbf{H}, \mathbf{E}, \mathbf{J}_p)\|_{\mathcal{C}^0([0,T],H^{s+1}(\Omega)^9)}\right)$$

Nearfield enhancement of a gold nanosphere (R=20 nm)

- Incident field: pulse modulated plane wave propagating along Oz

$$\mathbf{E}_{inc}(t) = \sin\left(2\pi f_c(t-4\tau)\right) \mathrm{e}^{-\left(\frac{t-4\tau}{\tau}\right)^2} \mathbf{e}_x$$

ε_∞	ω_0 GHz	γ_d GHz	f_c GHz	τ sec
1	1.19×10^7	1.41×10^5	4.5×10^5	2×10^{-15}

Nearfield enhancement of a gold nanosphere (R=20 nm)

Mesh	# tetrahedra	$L^1_{\mathbb{P}_1}$	$L^1_{\mathbb{P}_2}$
M1	153,517	1.1081×10^{-8}	8.3051×10^{-9}
M2	881,154	7.6520×10^{-9}	6.6986×10^{-9}
M3	2,338,433	6.6025×10^{-9}	Not available

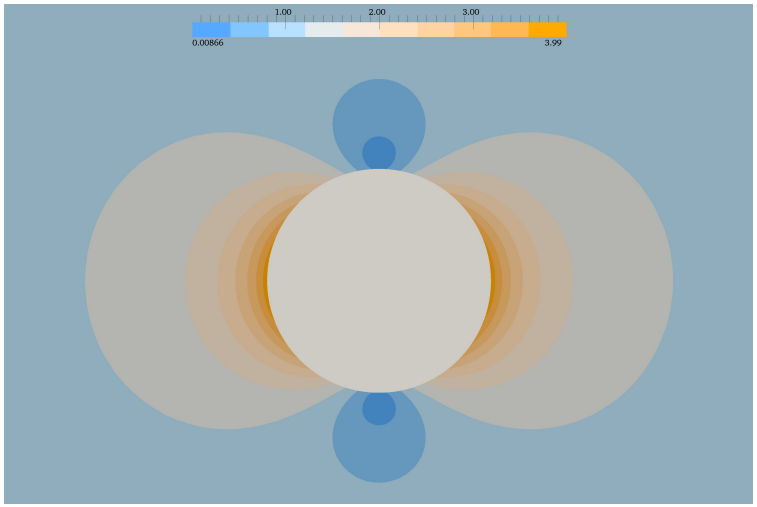

DGTD-$\mathbb{P}_2$ solution (M2 mesh)

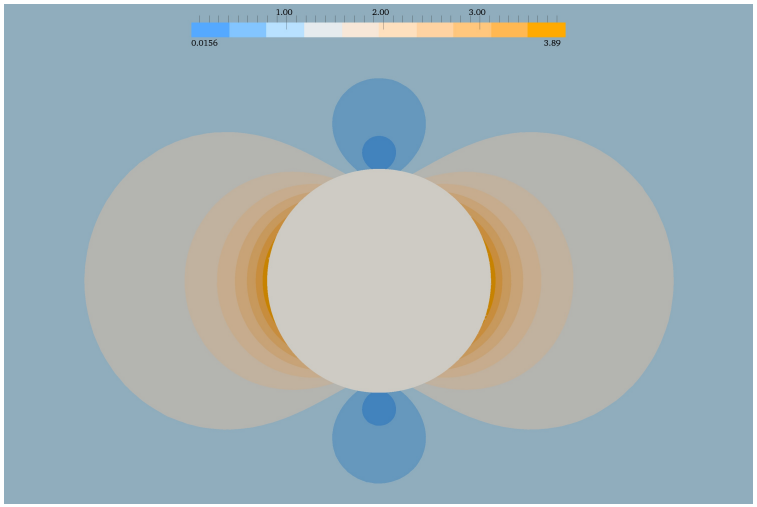

Mie solution

Comparison of DGTD and Mie solutions

Nearfield enhancement of a gold nanosphere (R=20 nm)

Mesh	# tetrahedra	$L^1_{\mathbb{P}_1}$	$L^1_{\mathbb{P}_2}$
M1	153,517	1.1081×10^{-8}	8.3051×10^{-9}
M2	881,154	7.6520×10^{-9}	6.6986×10^{-9}
M3	2,338,433	6.6025×10^{-9}	Not available

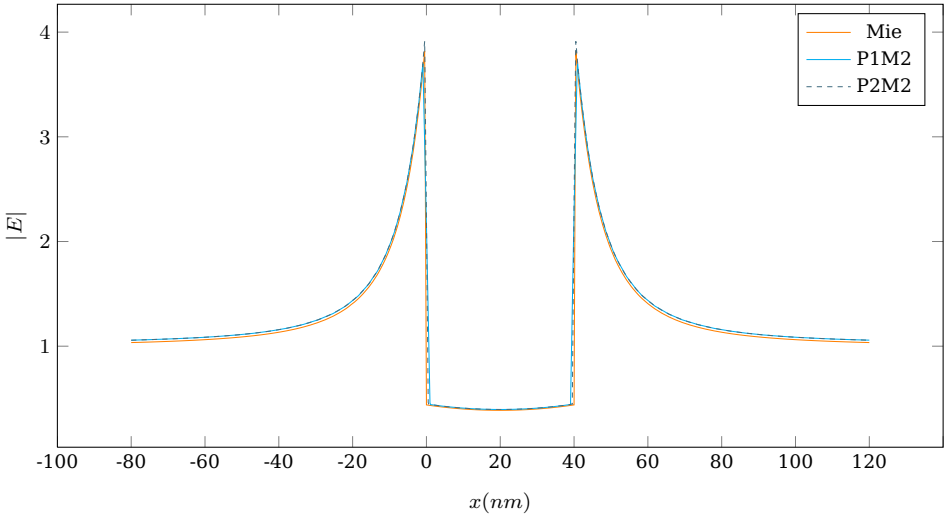

Mie and DG 1D plot of the electric field modulus across the dispersive gold nanosphere for various meshes and approximation ordrers

L-shaped nanospheres waveguide

- The L-shaped guide consists of 7 50 nm diameter Au spheres in vacuum
- 75 *nm* center-to-center spacing
- 550 nm$\times$750 nm$\times$400 nm parallelepipedic domain
- Silver-Müller absorbing boundary condition
- DGTD-$\mathbb{P}_p$ and DGTD-$\mathbb{P}_p\mathbb{Q}_k$ methods

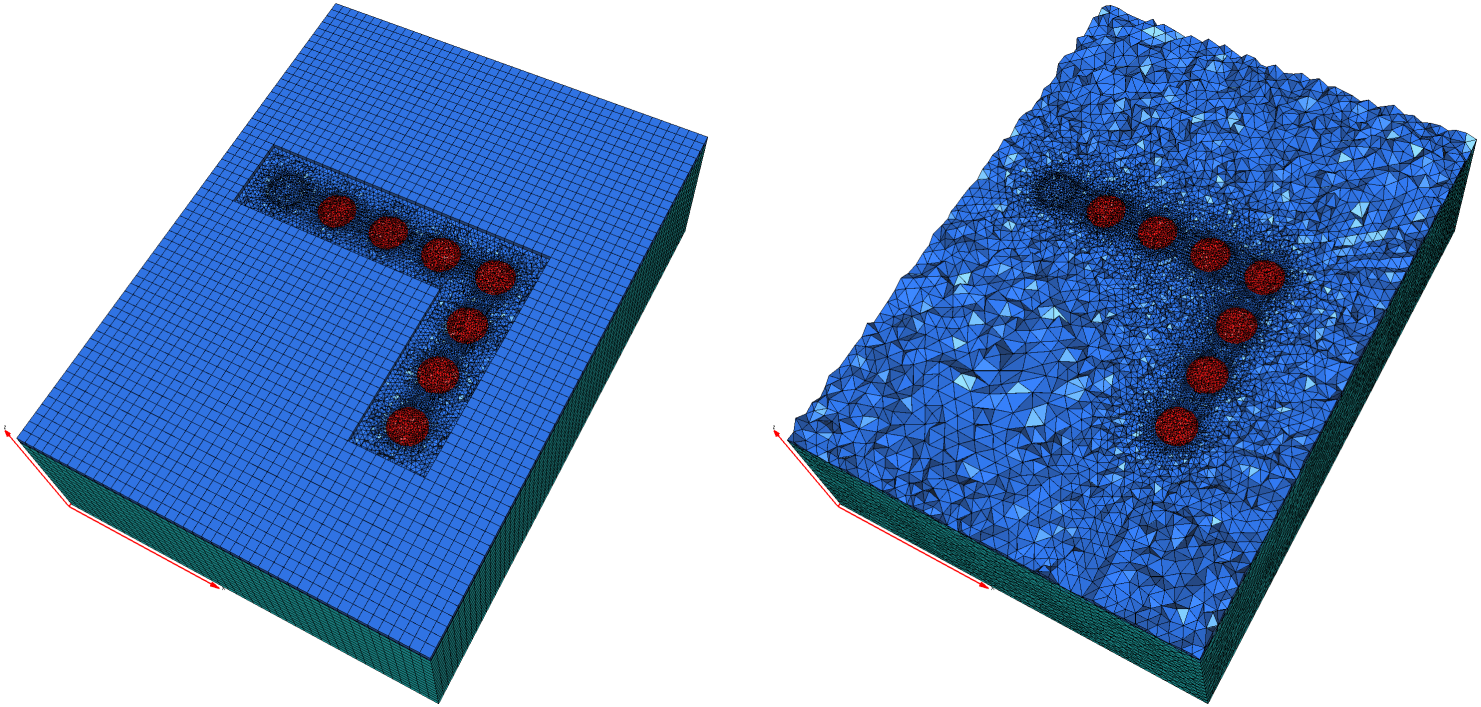

Partial views of the tetrahedral and hybrid hexahedral-tetrahedral meshes

K.-Y. Jung and F. L. Teixeira and R. M. Reano
Au/SiO_2 nanoring plasmon waveguides at optical communication band
J. Lightwave Technol., Vol. 25, No. 9, 2007

F. L. Teixeira
Time-domain finite-difference and finite-element methods for Maxwell equations in complex media
IEEE Trans. Antennas and Propag., Vol. 56, No. 8, 2008

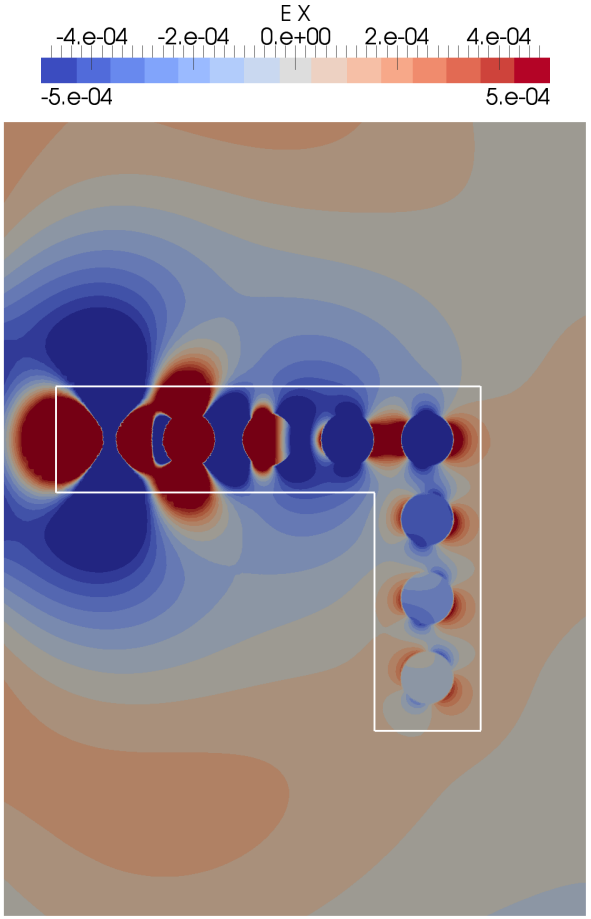

Contour lines of the E_x component of the electric field
DGTD-$\mathbb{P}_2\mathbb{Q}_2$ solution at time $t = 6.02$ fs

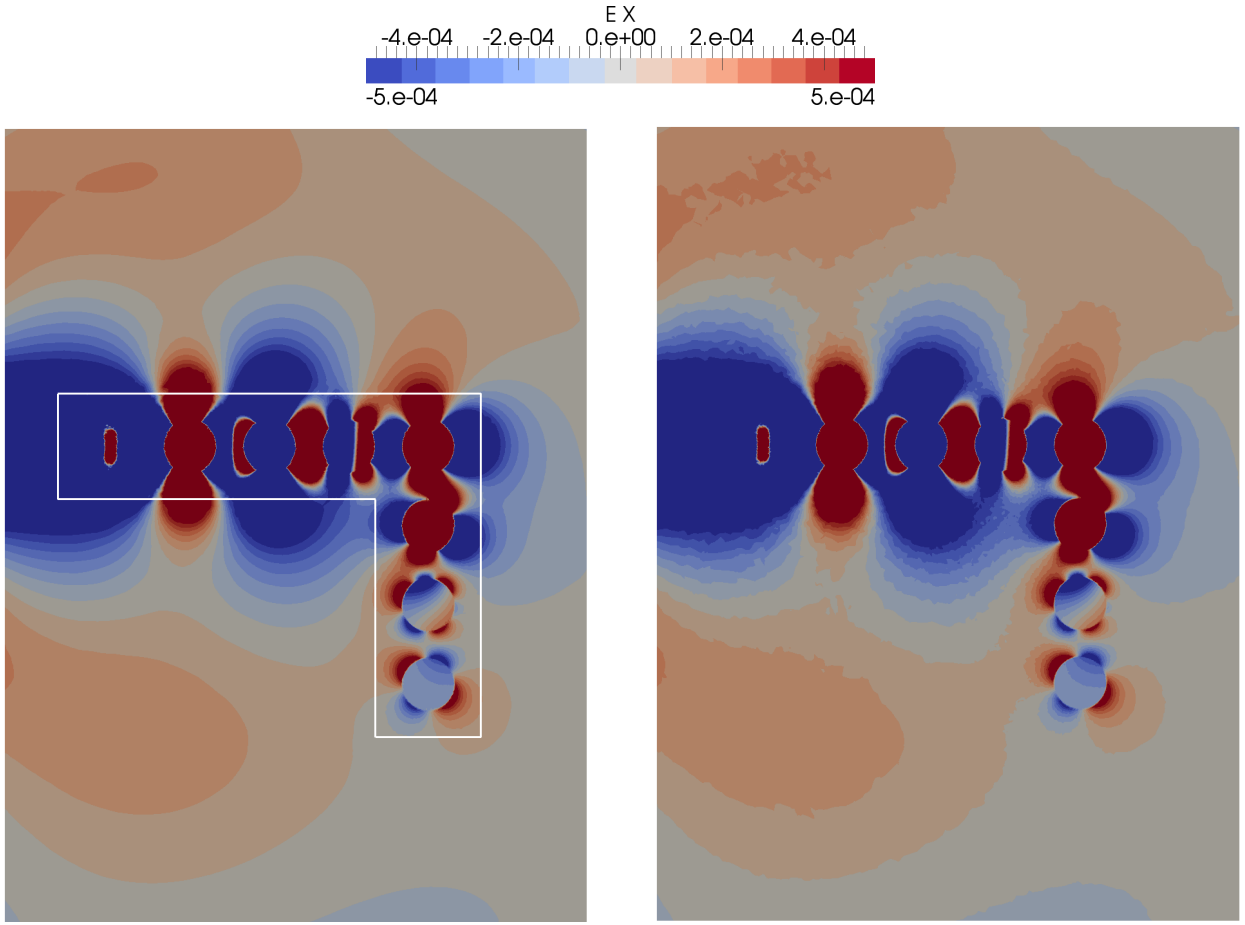

Controur lines of the E_x component of the electric field
DGTD-$\mathbb{P}_2\mathbb{Q}_2$ (left) and DGTD-$\mathbb{P}_2$ (right) solutions at final time $t_f = 34.13$ fs

L-shaped nanospheres waveguide

- Dipolar source 75 nm away from the center of the first sphere in the guide

$$J_x((x,y,z,t) = \delta(x-x_s, y-y_s, z-z_s)f(t) \quad \text{with} \quad f(t) = \left(1 - e^{-(t/\alpha)^2}\right)\sin(2\pi f_c t)$$

- Central frequency is $f_c = 622.65$ THz
- $\gamma = 2.5 \times 10^{16}$ and $\alpha = 2.5833$ fs
-
- DGTD-$\mathbb{P}_p$ and DGTD-$\mathbb{P}_p\mathbb{Q}_k$ methods

-	# vertices	# tetra	# hexa	# d.o.f
DGTD-$\mathbb{P}_2$	222,175	1,306,356	0	13,063,560
DGTD-$\mathbb{P}_2\mathbb{Q}_2$	211,214	706,012	81,280	9,264,660

Characteristics of the tetrahedral and hybrid hexahedral-tetrahedral meshes

-	8 cores	16 cores	32 cores	64 cores	128 cores
DGTD-$\mathbb{P}_2$	11420 s (1.0)	5710 s (2.0)	2800 s (4.1)	1455 s (7.8)	762 s (15.0)
DGTD-$\mathbb{P}_2\mathbb{Q}_2$	5680 s (1.0)	2804 s (2.0)	1439 s (3.9)	848 s (6.7)	494 s (11.5)

Performance results: CPU time to reach 1 fs and parallel speedup (in parentheses)

L-shaped nanospheres waveguide

- Dipolar source 75 nm away from the center of the first sphere in the guide

$$J_x((x,y,z,t) = \delta(x-x_s, y-y_s, z-z_s)f(t) \quad \text{with} \quad f(t) = \left(1 - e^{-(t/\alpha)^2}\right)\sin(2\pi f_c t)$$

- Central frequency is $f_c = 622.65$ THz
- $\gamma = 2.5 \times 10^{16}$ and $\alpha = 2.5833$ fs
-
- DGTD-$\mathbb{P}_p$ and DGTD-$\mathbb{P}_p\mathbb{Q}_k$ methods

-	# vertices	# tetra	# hexa	# d.o.f
DGTD-$\mathbb{P}_2$	222,175	1,306,356	0	13,063,560
DGTD-$\mathbb{P}_2\mathbb{Q}_2$	211,214	706,012	81,280	9,264,660

Characteristics of the tetrahedral and hybrid hexahedral-tetrahedral meshes

-	8 cores	16 cores	32 cores	64 cores	128 cores
DGTD-$\mathbb{P}_2$	11420 s (1.0)	5710 s (2.0)	2800 s (4.1)	1455 s (7.8)	762 s (15.0)
DGTD-$\mathbb{P}_2\mathbb{Q}_2$	5680 s (1.0)	2804 s (2.0)	1439 s (3.9)	848 s (6.7)	494 s (11.5)

Performance results: CPU time to reach 1 fs and parallel speedup (in parentheses)

Closure

Development of a dedicated software suite for nanophotonics (V1.0)

DIOGENeS
DIscOntinuous GalErkin Nano Solver
http://www-sop.inria.fr/nachos/index.php/Main/Software

- 3D time-domain Maxwell equations
- Drude, Drude-Lorentz and generalized dispersion models
- High order polynomial interpolation
- Unstructured and hybrid cubic/tetrahedral meshes
- Affine and curvilinear elements
- DG schemes with centered or upwind numerical fluxes
- Leap-frog (2nd and 4th order) and optimized Runge-Kutta time schemes
- Hybrid MIMD/SMIMD parallelization based on MPI/OpenMP

Ongoing efforts

- Non-local dispersion effects (hydrodynamic model)
- Non-linear Maxwell equations (Kerr type media)

Possible research directions within HOSCAR

- There are plenty of problems in nanophotonics that are heterogeneous and multiscale
- Optimization (structural and topological) has to be considered as one of the the next steps
- Exploit MHM methods in this context

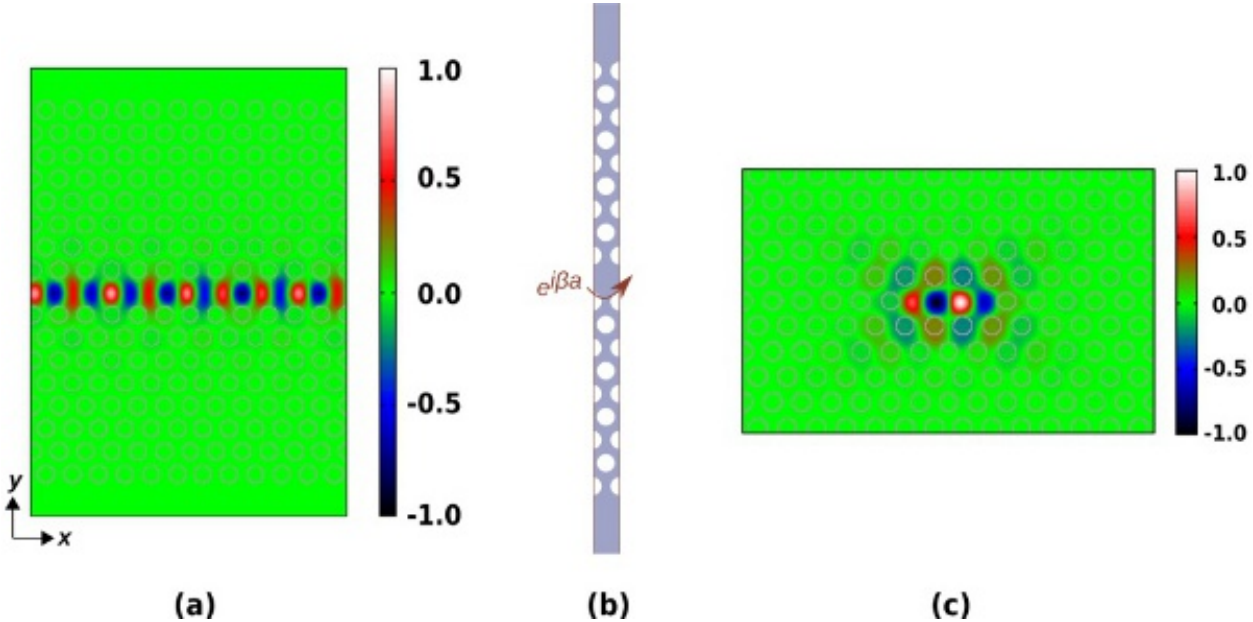

From: Two-dimensional photonic crystal micro-cavities for chip-scale laser applications
Recent optical and photonic technologies, InTech publishing, 2010

Thank you for your attention!

Possible research directions within HOSCAR

- There are plenty of problems in nanophotonics that are heterogeneous and multiscale
- Optimization (structural and topological) has to be considered as one of the the next steps
- Exploit MHM methods in this context

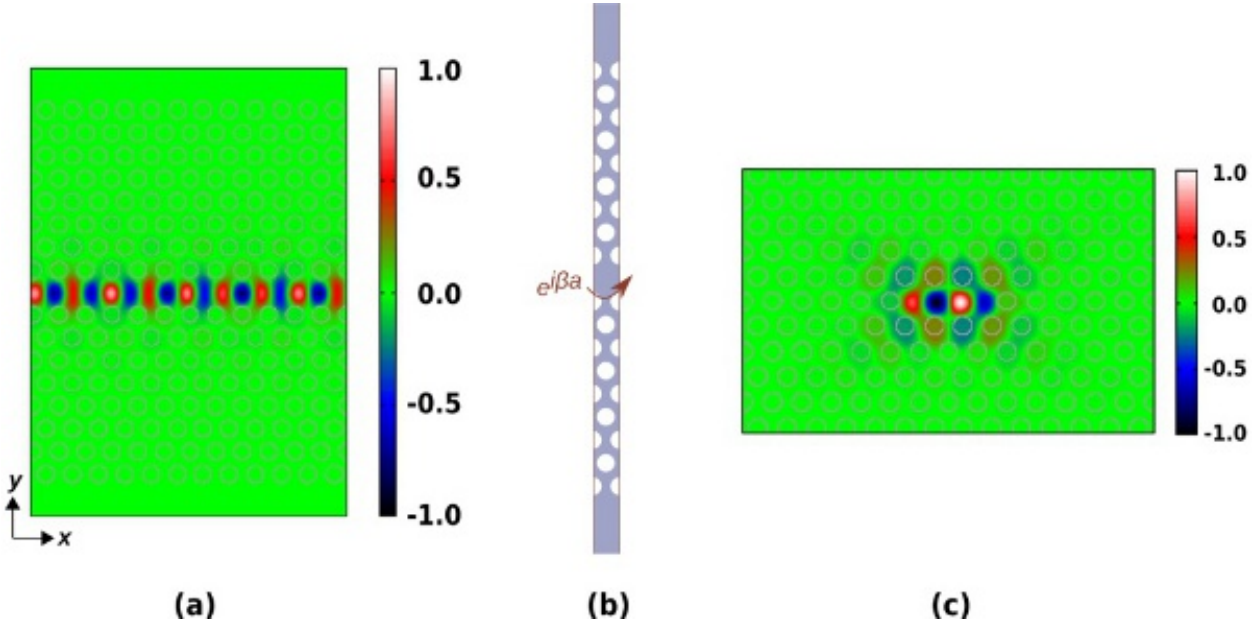

From: Two-dimensional photonic crystal micro-cavities for chip-scale laser applications
Recent optical and photonic technologies, InTech publishing, 2010

Thank you for your attention!